Wire array Z-pinch experiments on the MAGPIE generator, simulations and theory.

M. G. Haines, S. V. Lebedev, J. P. Chittenden, R. Aliaga-Rossel, S.N. Bland and A. E. Dangor.

The Blackett Laboratory, Imperial College, London SW7 2BZ, U. K.

Fast z-pinch implosions are an effective way of converting stored electrical energy into x-rays. Among other applications [1], pinch x-ray sources are used to energise hohlraums to blackbody temperatures of ~ 150 eV[2] for experiments relevant to the indirect drive ICF program and other radiation-hydrodynamic studies. Power levels of up to ~ 200 TW[3] have been obtained by the use of cylindrical arrays of large numbers (~240) of thin metallic wires as a z-pinch load. There is a general understanding that the high degree of symmetry of the load in large wire number shots is a key factor in attaining high X-ray power [4].

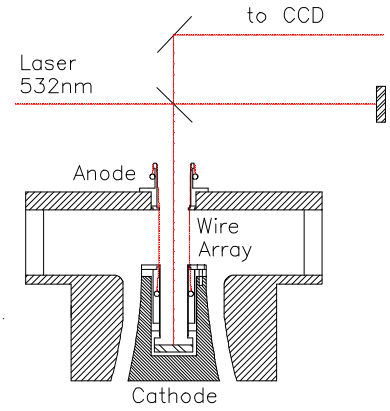

Fig. 1. The schematic of the wire array design to allow measurements of the azimuthal structure of the plasma by end-on interferometer.

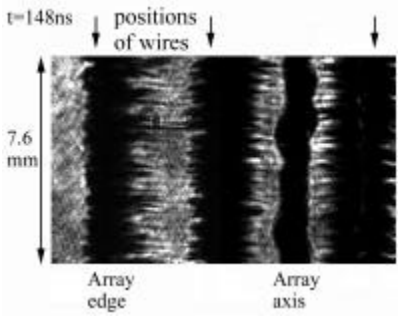

Fig. 2. Schlieren image of the 8 wires array showing m=0-like instabilities in wires and precursor pinch on the array axis at t=148 ns.

In this paper we present measurements of the dynamics of plasma formation in wire-array z-pinches. The experiments were carried out on the MAGPIE (Mega Ampere Generator for Plasma Implosion Experiments) generator [5] with current rising up to 1 or 1.4 MA in 240 ns (10% to 90% rise-time is 150 ns). Figure 1 shows a schematic of the wire array load used in this experiment. The 1.6 cm diameter 2.3 cm long annular wire array is mounted between the live cathode and the anode plate. Eight current-return posts are situated on a diameter of 15 cm. The design allows both end-on and side-on diagnosis of the whole array. Experiments were performed with arrays of 8, 16, 32 and 64 aluminium wires of 15 μm diameter. A frequency doubled Nd-YAG laser (532 nm) with SBS pulse compression (0.4 ns) was used for optical probing and CCD (charge coupled device) cameras were used as the recording media.

Figure 2 shows a typical side-on schlieren photograph of the array with 8 wires at 148ns after the current start. It is seen that the coronal plasma expands with the development of an m=0 like instability with axial wavelength of ~0.5 mm. These instabilities are similar to those observed in single wire z-pinches [6,7,8], but the global magnetic field modifies the instability pattern, which is no longer symmetric around each wire axis. Comparison of these instabilities in different wires shows that they are not correlated during the initial stage of the discharge. This supports assumptions used in the heuristic model of the wire array z-pinch [9] to determine subsequent average amplitude of seed perturbations at shell formation.

From the schlieren photographs, taken at different times after the current start, it is possible to determine the dynamics of the coronal plasma expansion from the wires in both the radial and azimuthal directions. The increasing size of the plasma around wires at the edge of the array provides measurements of velocities of the inward (to the array axis) and outward radial motion of the coronal plasma (Fig.3).

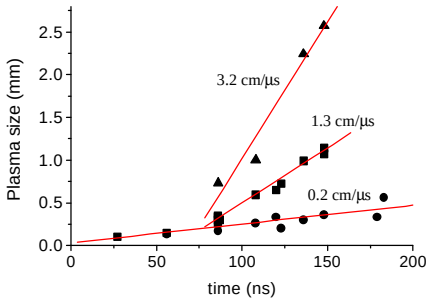

Fig. 3. Coronal plasma size in azimuthal (■) and radial (▲ - inward, ● - outward) directions as a function of time.

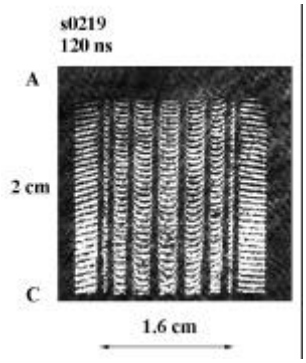

Fig. 4. Interferometer side-on image of the array

Typical side-on interferogram taken from array with 16 wires at 120 ns (half of the implosion time) is shown in Fig.4. The interference fringes between the wires are visible up to a distance of about 0.3 mm from the wire centre. For the wires near the centre of the array measurement of the interference fringes shift yields the distribution of $<n_e l>$ versus distance from the wire position, the maximum value being of $3x10^{17}$ cm^{-2} at 0.3 mm from the wire centre.

Fig. 5 shows end-on interferogram and a shadowgram for a 16 wire array. A fringe shift of 1 fringe corresponds to an electron number density of $9.1x10^{16}$ cm^{-3} for a probing path parallel to the pinch axis of 2x2.3 cm long. At times less than 60 ns the plasma density inside the array is below the sensitivity of the interferometer ($n_e < 3x10^{16}$ cm^{-3}). Note that the delay in the start of plasma expansion is the same for the end-on and side-on measurements. After this time the plasma is observed inside the array in the form of radially directed streams.

For an array with 32 wires results of simultaneous end-on and side-on laser probing, obtained at 112 ns in the same discharge, are shown in Fig.6a. The coronal plasma after merging has formed a continuous but axially non-uniform shell, the inner boundary of which at this moment has reached a radius of r/r_0 ~0.35. The side-on interferogram shows that plasma around the wires has a much higher density and that the residual wires are still in their initial positions. End-on images, obtained later in the discharge (Fig. 6b) show that the gradients of plasma density almost everywhere inside the array, including region around the array axis, are too high to allow the probing laser beam to pass through the plasma. The coronal plasma is accelerated radially inwards from the wires by the pressure of the global magnetic field and arrives at the axis before the array implosion, where it accumulates forming the precursor pinch. In arrays with small number of wires (~10) precursor was detected in earlier experiments [10,11].

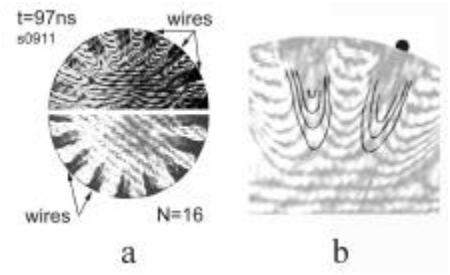

Fig.5. End-on interferogram and shadowgram of the same half (mirror reflected) of a 16 wire array (a), and electron number density contours (b) corresponding to multiples of n_e = $9x10^{16}$ cm^{-3}.

From the radial streak pictures (Fig.7) optical emission on the array axis starts at 120 - 130 ns for arrays with 8, 16 and 32 wires. For 64 wires this time is ~150 ns. Emission is observed from a well defined region of about 1 mm in diameter, which is practically constant in time.

The interferogram on Fig. 6b shows precursor just after its formation (126 ns). The maximum density found from Abel inversion is $5x10^{18}$ cm^{-3} and the precursor pinch diameter measured at the half of the density maximum is 0.6 mm. It is seen from the end-on laser probing images taken in the same shot (Fig. 6b) that the precursor pinch is surrounded by a lower density plasma of ~5 mm diameter.

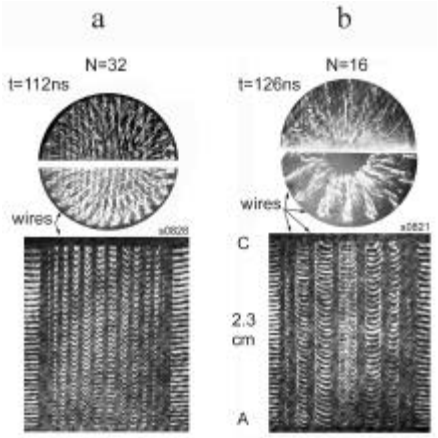

Fig. 6. End-on interferograms (upper) and shadowgrams (lower) obtained simultaneously with side-on interferograms (bottom) of arrays with 32 (a) and 16 (b) wires.

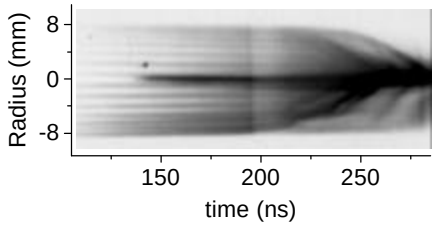

Fig. 7. Radial streak photograph of 32 wire array (1 MA) showing optical emission from the precursor pinch on the array axis.

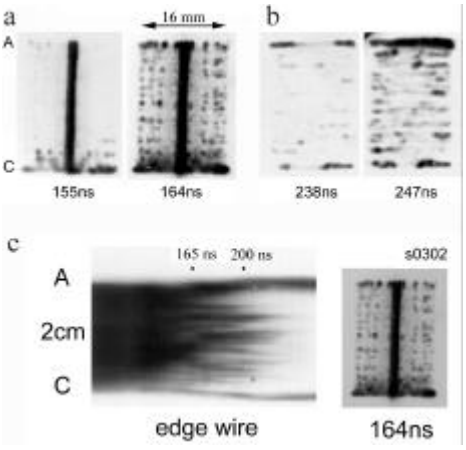

Fig. 8. Soft x-ray images showing formation of correlated bright spots due to the development of a global instability in arrays with 16 (a) and 64 (c) wires, and an axial streak photograph of the edge wire (for 16 wires).

On gated soft x-ray images (Fig. 8) the precursor is observed from ~110 ns until the stagnation of the array, as a homogeneous plasma column with the same diameter of about 1 mm which slowly increases in time at a rate of ~$2x10^6$ cm/s.

The precursor formation time is almost the same for different numbers of wires and agrees well with simulations and an inward velocity of ~15 cm/μs of the low density coronal plasma found from end-on measurements and with the observed 60 ns delay in the start of this fast motion of the coronal plasma. The corresponding kinetic energy of the aluminium ions arriving at the axis is ~ 3 keV. Thermalisation of this kinetic energy at stagnation and equipartition with electrons results in a relatively high temperature of the precursor plasma as supported by x-ray gated images, which are recorded with 5 μm polycarbonate filter, transmitting photons with energy more than ~200 eV.

During the later stages of implosion, starting at time t/t_{imp} ~ 0.7 - 0.8 (where t_{imp} is the calculated time of implosion), the development of a global m=0 instability, driven by the global magnetic field, is observed [12] by a number of diagnostics. Soft x-ray gated images at these times show formation of a number of bright spots at the initial radial positions of wires (Fig. 8). These bright spots are formed on all wires and their axial positions are correlated between different wires. The axial spatial separation between the spots varies slightly with number of wires in the array and is between 1.7 and 2.3 mm.

Axial streak photographs with the slit oriented in the z-direction along the wires at the edge of the array (Fig. 8c) show that the emission starts to be non-uniform with the same characteristic spatial scale of 1 - 2 mm at the time of the instability development.

The strongest candidate for the observed instability is the Rayleigh-Taylor instability in a plasma accelerated by the magnetic pressure [13]. A heuristic model by Haines [9] suggests a scaling for the seeded level of radial perturbations, δ_0, with number of wires as $\delta_0 \propto N^{-1/2}$, due to averaging of the non-correlated MHD instabilities which initially develop in individual wires. For the classical RT instability seeded perturbations will grow linearly as $\delta=\delta_0 \exp(\int\gamma(t)dt$, where $\gamma=(kg)^{1/2}$ with $k=2\pi/\lambda$ and g is the acceleration. The number of instability e-foldings, $G\equiv\int\gamma dt$, at the time when perturbations reach a fixed amplitude δ_* will be

related to the number of wires according to $\exp(-G)=\delta_0/\delta_* \propto N^{-1/2}$. (1)
The calculated value of *G* increases with the number of wires from 5.6 to 7.1 and the plot in Fig. 9 shows that the experimental data agrees reasonably well with the above scaling law.

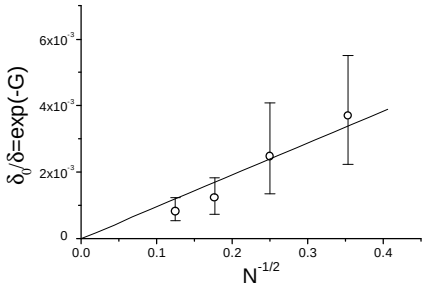

Fig. 9. Fit of the experimental data to the scaling law of equation (1). The error bars are due to uncertainty in the time of appearance of bright spots, equal to half of the x-ray camera inter-frame separation.

Diagnosis of the inner surface of the R-T unstable imploding plasma "shell" by laser probing in arrays with equally spaced wires is virtually impossible due to overlapping of plasmas from closely positioned wires and only axially correlated gaps in wires can be seen [12]. In an attempt to overcame this difficulty and observe instability structure more clearly, experiments with array which consist of 4 groups of 4 wires in each group (Fig. 10) were carried out. The radial part of ***JxB*** force acting on wires in this configuration is the same as in array with equally spaced wires [14], and the experimentally observed implosion time was the same as for a 16 wire array. The laser probing (Fig. 10) clearly shows development of the Rayleigh-Taylor instability with the same axial wavelength of 1.7 mm, and with characteristic spikes on the outer surface and smooth modulation consistent with the presence of bubbles on the inner surface.

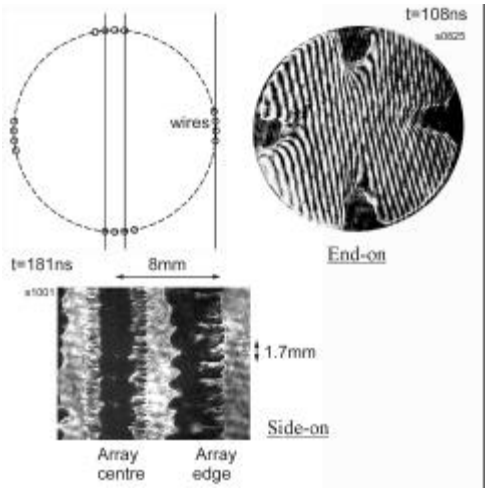

Fig. 10. Side-on laser shadow image showing development of Rayleigh-Taylor instability with λ = 1.7 mm during implosion of 4x4 wire array and end-on interferogram taken at earlier time. Orientation of the array in respect to the direction of probing is shown at the top. Spacing between wires in each group correspond to array with 64 wires.

This work was supported by EPSRC Grant No. GR/M20525 and by U.S. Department of Energy Contract No. DE-FG03-98DP00217.

1 N.R. Pereira and J. Davis, J. Appl. Phys. **64**, R1 (1988).
2 M.K. Matzen, Phys. Plasmas **4**, 1519 (1997).
3 R.B. Spielman et al., Phys. Plasmas **5**,2105 (1998).
4 T.W.L. Sanford et al., Phys. Plasmas **4**,2188 (1997).
5 I.H. Mitchell et al., Rev. Sci. Instrum. **67**, 1533 (1996).
6 D. Mosher and D. Colombant, Phys. Rev. Lett. **68**, 2600 (1992).
7 D. Kalantar and D. Hammer, Phys. Rev. Lett. **71** 3806 (1993).
8 F.N. Beg et al., Plasma Phys. Control. Fusion **39**, 1 (1997).
9 M.G. Haines, IEEE Trans. Plasma Sci. **26**,1275 (1998).
10 C. Deeney et al., Phys. Rev. E, **51**, 4823 (1995).
11 E.J. Yadlowsky et al, Phys. Plasmas **3**, 1745, 1996.
12 S. V. Lebedev et al., Phys. Rev. Lett. **81**, 4152 (1998).
13 T.W. Hussey, N.F. Roderick, D.A. Kloc, J. Appl. Phys. **51**, 1452 (1980).
14 F.S. Felber, N. Rostoker, Phys. Fluids, **24**, 1049 (1981).